

Clinical Cardiovascular Research

Research Article

Significance of Left Ventricular Strain in Traditional Cardiac Risk Factor Population

Akhil Mehrotra^{1*}, Mohammad Shaban², Faiz Illahi siddiqui², Shubham Kacker², Mohammad Shadab², Naveen Chandra²

¹Chief, Pediatric, and Adult Cardiology, Prakash Heart Station, Nirala Nagar, Lucknow, UP, India.

²Cardiac Technician, Prakash Heart Station, Nirala Nagar, Lucknow, UP, India.

³Senior Interventional Cardiologist, Lucknow, India.

***Corresponding Author:** Dr. Akhil Mehrotra, Chief, Non Invasive Cardiologist, Pediatric and Adult Cardiology. Prakash Heart Station, D-16 Nirala Nagar- 226020, Lucknow, UP, India.

Received Date: 22 August 2025; **Accepted Date:** 12 September 2025; **Published Date:** 16 September 2025

Copyright: © 2025 Akhil Mehrotra, this is an open-access article distributed under the Creative Commons Attribution License, which permits unrestricted use, distribution, and reproduction in any medium, provided the original work is properly cited.

Abstract

Background: 4-Dimensional XStrain speckle tracking echocardiography (4DXStrainSTE) is an advanced cardiac imaging technique that synthesizes speckle tracking echocardiography (STE) data obtained from the apical three-chamber (3CH), four-chamber (4CH), and two-chamber (2CH) views, thereby enabling a comprehensive evaluation of multiple left ventricular strain parameters (MLVSP) within a three-dimensional framework.

Methods: This study aimed to evaluate the impact of cardiovascular risk factors (CVRFs) on MLVSP using 4DXStrainSTE. Nine strain parameters were analyzed: global circumferential strain (GCS), global circumferential strain rate (GCSR), global radial strain (GRS), and global radial strain rate (GRSR) at the mitral valve (mv) and papillary muscle (pap) levels, along with global longitudinal strain (GLS). A total of 500 Indian adults (aged 18–60 years; both sexes) were enrolled. Participants were categorized into four CVRF Risk Categories (1, 2, 3, and 4) according to the cumulative number of risk factors. The inclusion criterion was a 4-dimensional left ventricular ejection fraction (4D-LVEF) > 50%.

Results: The effect of CVRF on strain parameters was determined using trend and linearity analyses. Trend analysis across CVRF categories revealed a significant decline in GLS, GCS at the pap level, and GCSR at the mv level. Pearson's correlation demonstrated mild-to-moderate linear associations across MLVSP, and multivariate regression analysis identified significant associations of GLS and GCSR at the mv level with GLS across the risk categories.

Conclusion: To the best of our knowledge, this is the first study to provide a comprehensive evaluation of the impact of CVRFs on MLVSP in individuals with preserved ejection fraction.

Keywords: 4DXStrain, Speckle tracking echocardiography, 4D-LVEF%, Cardiovascular risk factors, Trend analysis.

Introduction

Currently, global longitudinal strain (GLS) assessment via two-dimensional speckle tracking echocardiography (2D STE) remains one of the most extensively investigated techniques worldwide [1]. The American Society of Echocardiography recommends a normal GLS value of $> -20 \pm 2\%$ [2]. Three-dimensional speckle tracking echocardiography (3D

STE) enables single-apical acquisition of the left ventricle, thereby reducing acquisition time and allowing a comprehensive evaluation of strain parameters [3]. However, its clinical application is constrained by suboptimal temporal and spatial resolution, which can impair tracking accuracy. In addition, multi-beat acquisitions may introduce stitching artifacts

between sub-volumes, further compromising speckle tracking analysis [4,5].

4DXStrainSTE is an innovative and advanced imaging modality that integrates Tomtec GMBH's 3D/4D imaging platform with Beutel™ computational technology [6]. It synthesizes STE data from apical 3CH, 4CH, and 2CH views to achieve a comprehensive three-dimensional reconstruction of left ventricular (LV) strain parameters. By capitalizing on the superior temporal and spatial resolution of 2D imaging, this technique effectively mitigates the inherent limitations of full-volume 3D STE [7]. While single-plane 3D echocardiography still suffers from lower resolution compared to 2D imaging [8], 4DXStrainSTE overcomes these constraints and offers an accessible, cost-efficient, and user-friendly solution for LV strain analysis.

Previous studies have documented the impact of cardiovascular risk factors (CVRFs) on GLS [9,10], though primarily using 2D STE. A thorough literature search revealed no prior studies that comprehensively evaluated the influence of CVRFs on multiple LV strain parameters (MLVSP) through rigorous statistical techniques—namely, trend analysis, Pearson's correlation, and multivariate regression for linearity assessment. This investigation was therefore designed to

address this important methodological gap.

Method

Study Center

This original research was conducted over a 28-month period (September 2021 to December 2023) at Prakash Heart Station, Lucknow, Uttar Pradesh, India.

Ethical Approval

Ethical approval was granted by the Institutional Ethics Committee of Prakash Heart Station (Approval No. IEC/PDC/PHSD/2021:01,02). All participants provided written informed consent after receiving a detailed explanation of the study's aims. The research procedures were carried out in alignment with the International Conference on Harmonisation-Good Clinical Practice (ICH-GCP) standards and adhered to the ethical principles set forth in the Declaration of Helsinki.

Study Population

This was a single-center, observational, prospective study involving 500 Indian adults aged 18–60 years, of both sexes. Participants were classified into four CVRFs categories: category 1, 2, 3, and 4 (Figure 1).

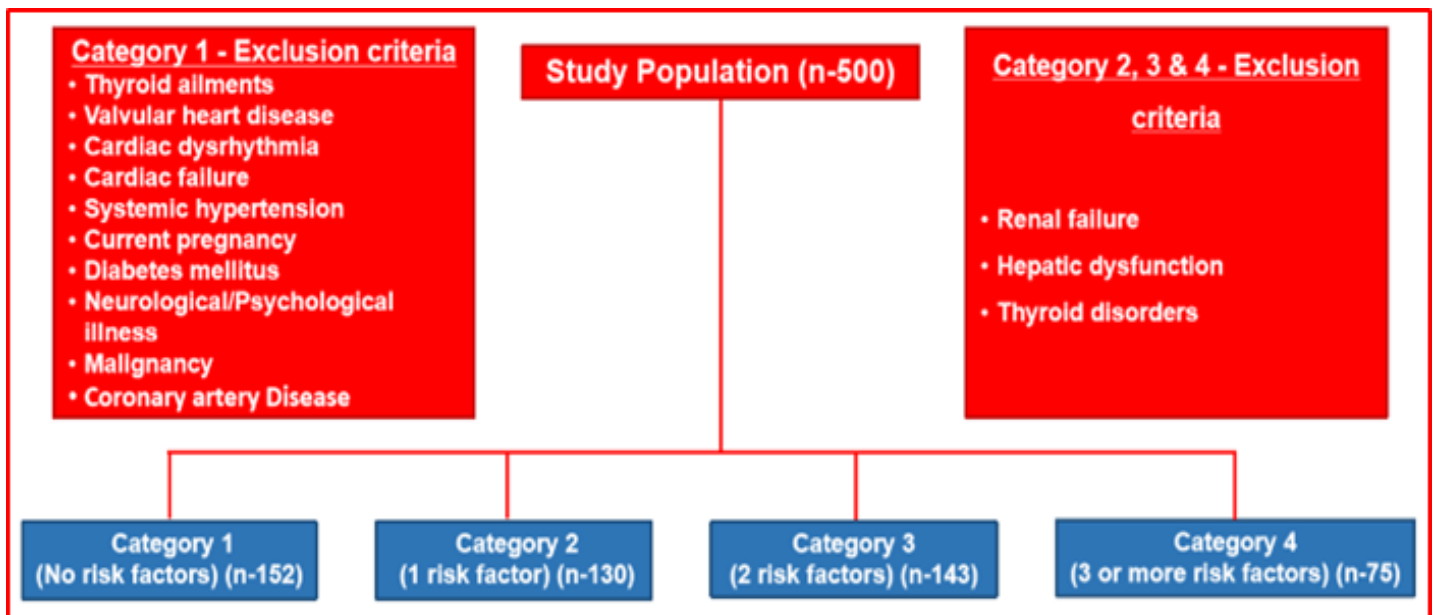


Figure 1: Classification steps of the study design.

Category 1

This group included 152 healthy individuals (aged 18–60 years; both sexes) without any CVRFs, exhibiting normal resting electrocardiograms (ECG), 4DXStrainSTE findings with 4D-LVEF > 50%, and negative treadmill stress tests (TST).

Category 2, 3 & 4

This cohort comprised 348 adults (aged 18–60 years; both

sexes) with one or more CVRFs, all in sinus rhythm and exhibiting a 4D-LVEF > 50%. Inclusion criteria stipulated that all participants maintain a 4D-LVEF ≥ 50%, as quantified by 4DXStrainSTE. Comprehensive clinical and medical assessments were conducted by a cardiac physician, with meticulous documentation of the CVRF profile for each participant.

Cardiovascular Risk Factors

- Cardiovascular disease:

(i) CAD: history of myocardial infarction, stable/unstable an-

gina, acute coronary syndrome, or percutaneous coronary intervention (PCI)

- (ii) CVA (cerebrovascular accident)
- (iii) PAD (peripheral arterial disease)

- Diabetes mellitus
- Hypertension
- Dyslipidemia
- Obesity
- Smoking

Definitions of all risk factors adhered to current guidelines [11–15].

Echocardiography

All participants underwent comprehensive cardiac evaluation using conventional two-dimensional (2D) transthoracic echocardiography and 4DXStrainSTE. Examinations were conducted on the MY LAB X7 4D XStrain system (ESAOTE, Italy) equipped with a 1–5 MHz transducer. All acquisitions were performed by the experienced study authors, with measurements obtained in accordance with the American Society of Echocardiography guidelines [16].

Conventional Echocardiography

Two-dimensional, M-mode, pulse-wave Doppler (PWD), continuous-wave Doppler (CWD), and tissue Doppler imaging (TDI) modalities were employed to evaluate standard cardiac parameters, including left ventricular (LV) volumes, systolic and diastolic function, LV mass, left ventricular ejection fraction (LVEF%), cardiac output (CO), cardiac index (CI), early diastolic (E) and late diastolic (A) velocities, E/A ratio, early myocardial relaxation velocity (E'), and the E/E' ratio.

4-Dimensional X-Strain Echocardiography Image Acquisition

Apical 4CH, 3CH, 2CH, and short-axis (SX) views at the mitral valve (mv) and papillary muscle (pap) levels were obtained (Figure 2). Each cine loop comprised at least three cardiac cycles, recorded at 40-75 frames per second (FPS) and stored digitally for offline analysis.

High-quality image acquisition was prioritized. Optimal ECG tracing was ensured by adjusting electrode placement on the chest and selecting the lead from the PHYSIO menu of the echocardiography system that yielded the smoothest waveform with well-defined R/Q waves and minimal noise. Traces exhibiting prominent P or T waves were avoided to prevent gating interference during 4DXStrainSTE acquisition. Participants were instructed to hold their breath at end-expiration to minimize translational and respiratory artifacts. The LV was positioned to fill the majority of the imaging sector, avoiding foreshortening. Particular care was taken to exclude papillary muscle bulges when tracing the endocardium.

High-quality short-axis views at the mv, pap, and LV apex levels were acquired to facilitate accurate computation of circumferential strain, circumferential strain rate, radial strain, and radial strain rate [17]. Clear delineation of cardiac bor-

ders was confirmed throughout the cardiac cycle.

Offline Analysis of Acquired Images

Speckle tracking analysis was performed offline using XStrain-4D™ (Esaote) software [18]. The LV endocardial and epicardial borders were automatically delineated from 13 equidistant tracking points, supported by the Aided Heart Segmentation (AHS) tool [18].

The Beutel computational platform, integrated into XStrain™ 4D, synthesizes STE data from apical 2D 3CH, 4CH, and 2CH views to reconstruct a 3D/4D LV model, enabling automated derivation of LV strain parameters [18]. A standardized 17-segment Bull's-eye plot was generated for visualization.

Strain Parameters Derived from XStrain 4DSTE

Nine strain parameters (Figure 3) were evaluated as outlined below:

GLS (%)

- 3CH view (%)
- 4CH view (%)
- 2CH view (%)

GCS

- mv level (%)
- pap level (%)

GCSR

- mv level (1/sec)
- pap level (1/sec)

GRS

- mv level (%)
- pap level (%)

GRSR

- mv level (1/sec)
- pap level (1/sec)

GLS and GCS are expressed as negative values, whereas GRS is represented as positive values. Similarly, strain and strain rate are denoted in % and 1/sec, respectively.

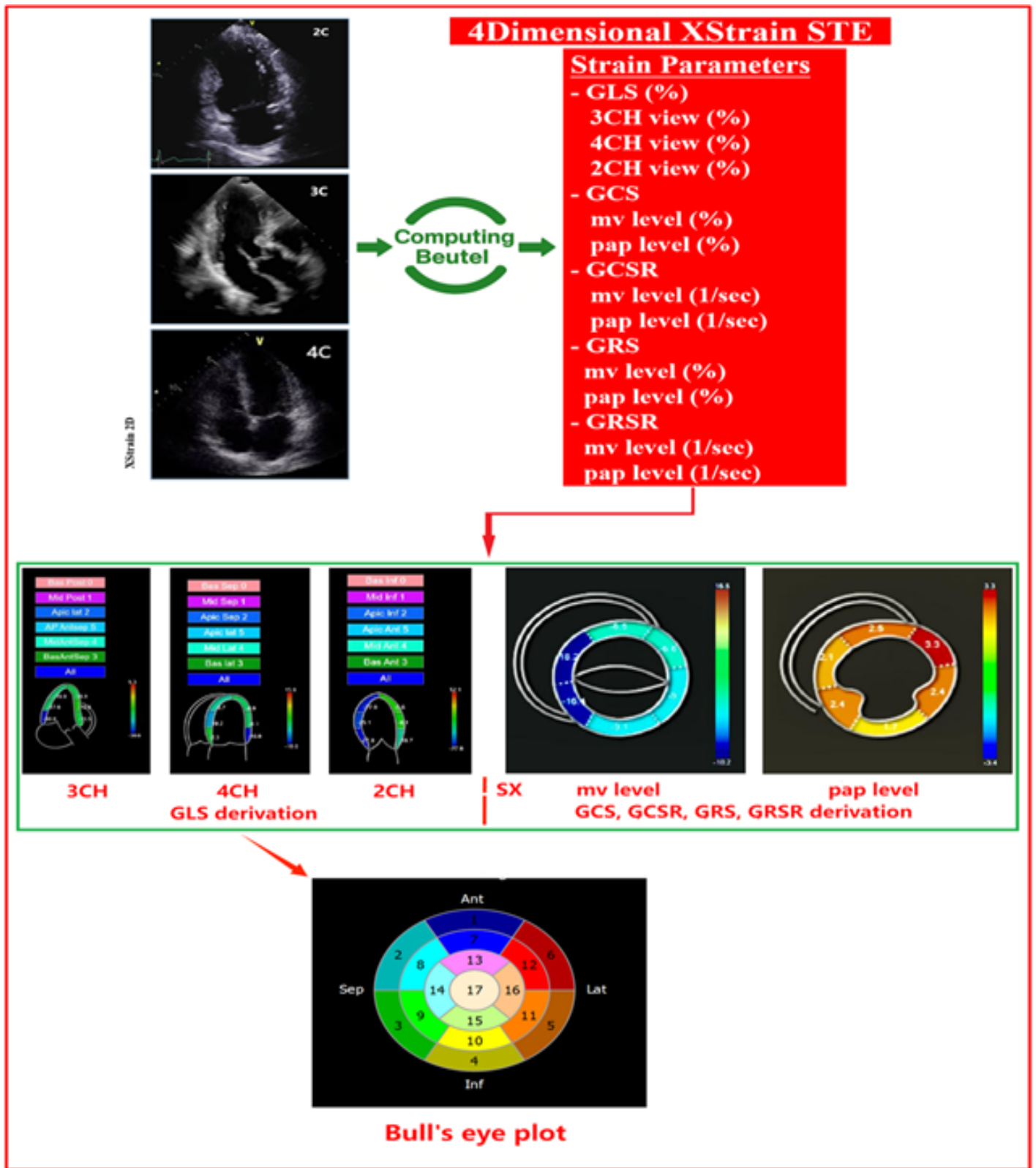


Figure 2: Illustration of 4DXStrain speckle tracking echocardiography. GLS, Global Longitudinal Strain; GCS, Global Circumferential Strain; GRS, Global Radial Strain; GCSR, Global Circumferential Strain Rate; GRSR, Global Radial Strain Rate.

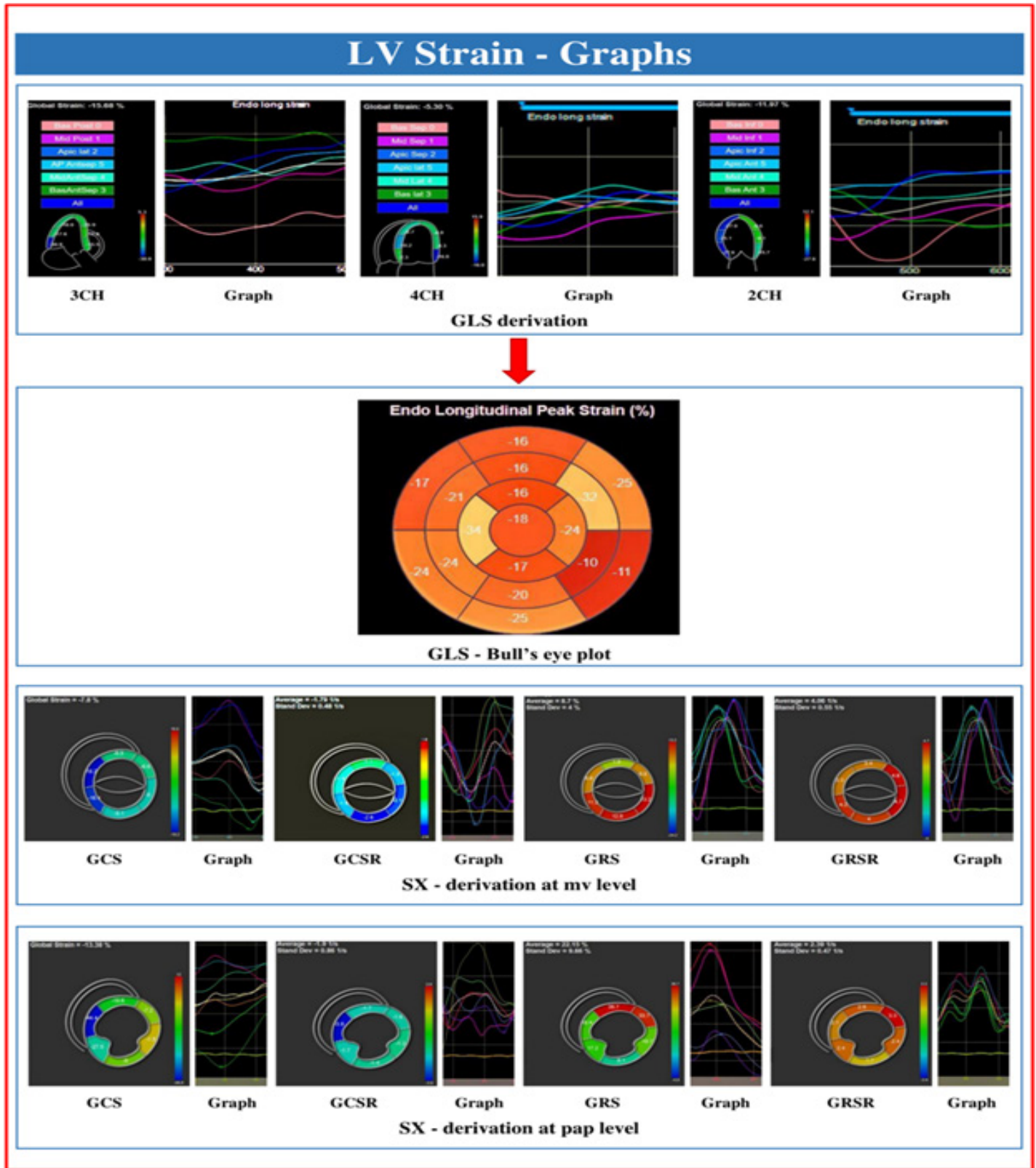


Figure3: Graphical representation of the nine LV strain parameters. GLS, Global Longitudinal Strain; GCS, Global Circumferential Strain; GRS, Global Radial Strain; GCSR, Global Circumferential Strain Rate; GRSR, Global Radial Strain Rate; mv, mitral valve; pap, papillary muscle; CH, chamber; SX, short axis view.

Statistical Analysis

Study subjects were categorized as follows:

- **Category 1:** Healthy individuals without CVRFs (Healthy group)
- **Category 2:** Individuals with only one CVRF
- **Category 3:** Individuals with two CVRFs
- **Category 4:** Individuals with three or more CVRFs

NB: The data of categories 2, 3, & 4 were pooled together for statistical analysis in Table 1 (Pooled group).

Statistical analyses were conducted using IBM SPSS Statistics, Version 26.0 (IBM Corp., Armonk, NY, USA). Graphical representations for trend analysis were created using Microsoft Excel 2013 (Version 15.0.558.1000; MSO 15.0.5589; 32-bit), included in Microsoft Office Professional Plus 2013.

- The **Shapiro–Wilk** test was conducted to assess the normality of distribution for continuous variables.
- Variables with normal distributions were expressed as **mean ± standard deviation**. The **Student's t-test** was applied to normally distributed data to determine the significance of differences between groups and risk categories (95% confidence intervals). Multiple independent t-tests comparing Risk Category 1 with Categories 2, 3, and 4 across various variables were conducted.
- For data that were not normally distributed, the **Mann–Whitney U test** was employed.
- **Levene's test** was applied to assess the homogeneity of variances.
- The **Tukey–Kramer** post hoc analysis was used to evaluate differences between parameters across CVRF risk categories.
- The **Kruskal–Wallis** test was utilized for data exhibiting unequal variances between groups.
- **Pearson's correlation coefficient** was calculated to measure the linear correlation between two data sets.
- **Trend & Multivariate regression analysis** was performed across Risk Categories 1–4.
- Continuous variables are expressed as mean ± standard deviation, whereas categorical variables are presented as frequencies and percentages (Table 1).

Statistical significance was defined as **p<0.05**, with **p<0.01** considered highly significant. Values with **p>0.05** were deemed not significant.

Results

Demographic Data

In Category 1 (Table 1), 152 healthy individuals were enrolled (103 males, 49 females). The mean age was 29.5 ± 10.24 years for males and 34.16 ± 9.95 years for females, with females being significantly older than males ($p < 0.01$). Males exhibited significantly greater weight, height, BMI, blood pressure (BP), and heart rate (HR) compared to females ($p < 0.01$).

In the pooled data, there were 348 participants (204 males, 144 females). The mean age of males was 49.85 ± 12.73 years, and that of females was 54.92 ± 12.58 years. Males had significantly higher weight, height, BMI, and diastolic BP (DBP) than females ($p < 0.01$), whereas systolic BP (SBP) and HR were significantly higher in females ($p < 0.01$).

Conventional Echocardiography Data

Routine two-dimensional echocardiography was employed to obtain conventional measurements.

In male subjects of Category 1 (Table 1), left atrial size, interventricular septal diameter (IVS d), left ventricular internal diameter in diastole (LVID d), left ventricular posterior wall diameter (LVPW d), left ventricular end-diastolic volume (LVEDV), LV mass in diastole (LV Mass d), cardiac output (CO), mitral E/A ratio, lateral wall tissue Doppler imaging (TDI) E' velocity, and 2D fractional shortening (FS) were significantly greater than in females ($p < 0.01$). Conversely, E-point septal separation (EPSS), lateral wall TDI E/E' ratio, and 2D left ventricular ejection fraction (2D-LVEF) were greater in females ($p < 0.01$, $p > 0.05$, and $p < 0.05$, respectively).

Pooled data values for EPSS, IVSd, LVID d, LVPW d, LVEDV, LV Mass d, CO, TDI E', and TDI E/E' ratio were significantly higher in males ($p < 0.01$, $p < 0.05$). In contrast, left atrial size, mitral E/A ratio, 2D-LVEF, and 2D-FS were significantly higher in females ($p < 0.01$).

4-Dimensional XStrain Speckle Tracking Data LV Strain Data

A comparative analysis of LV strain parameters between category 1 and the pooled category (Table 1) revealed a significant reduction in GLS and GCS at the pap level in the pooled category ($p < 0.001$ and $p = 0.01$, respectively), although GCSR at the pap level showed borderline significance ($p = 0.06$). Nevertheless, GCS at the mv level, global GRS at both mitral and papillary levels, and GCSR at the mv level were also lower in the pooled category; however, these differences did not reach statistical significance ($p > 0.05$). Meanwhile, GRSR at both the mitral and papillary levels was marginally higher in the pooled category, though this increase was not statistically significant ($p > 0.05$).

Demographic Data								
Variable	Category 1 (N-152)				Pooled category (N-348)			
	M (n-103)	F (n-49)	p		M (n-204)	F (n-144)	p	
	mn ± sd	mn ± sd	value	sign.	mn ± sd	mn ± sd	value	sign.
Age (years)	29.95 ± 10.24	34.16 ± 9.95	p<0.01	**	49.85 ± 12.73	54.92 ± 12.58	p<0.01	**
Weight (kg)	64.74 ± 11.28	57.51 ± 11.02	p<0.01	**	71.85 ± 11.41	63.33 ± 9.63	p<0.01	**
Height (cm)	164.68 ± 7.30	158.02 ± 7.60	p<0.01	**	167.12 ± 6.11	158.10 ± 6.26	p<0.01	**
BSA (M2)	3.42 ± 17.47	1.57 ± 0.17	p>0.05	NS	3.54 ± 16.67	2.72 ± 12.61	p>0.05	NS
BMI	23.85 ± 3.85	22.90 ± 3.29	p<0.01	**	25.37 ± 3.44	25.37 ± 3.80	p<0.01	**
SBP (mmhg)	118.39 ± 11.33	116.63 ± 11.76	p<0.01	**	132.30 ± 19.17	137.40 ± 19.76	p<0.01	**
DBP (mmhg)	77.14 ± 7.09	75.51 ± 7.30	p<0.01	**	82.05 ± 11.20	81.61 ± 10.98	p<0.01	**
HR (bpm)	77.83 ± 14.26	81.27 ± 16.34	p<0.01	**	75.60 ± 14.28	77.41 ± 15.56	p<0.01	**
Conventional Echocardiography Data								
Variable	Category 1 (N-152)				Pooled category (N-348)			
	M (n-103)	F (n-49)	p		M (n-204)	F (n-144)	p	
	mn ± sd	mn ± sd	value	sign.	mn ± sd	mn ± sd	value	sign.
EPSS (mm)	0.71 ± 0.63	0.73 ± 0.48	p<0.01	**	0.61 ± 0.31	0.60 ± 0.46	p<0.01	**
LA (cm)	2.86 ± 0.55	2.79 ± 0.50	p<0.01	**	3.35 ± 0.67	3.42 ± 1.81	p<0.01	**
IVS d (cm)	0.78 ± 0.18	0.72 ± 0.18	p<0.01	**	0.99 ± 0.21	0.95 ± 0.21	p<0.01	**
LVID d (cm)	4.80 ± 0.41	4.41 ± 0.74	p<0.01	**	4.71 ± 0.57	4.53 ± 0.60	p<0.01	**
LVPW d (cm)	0.80 ± 0.14	0.72 ± 0.16	p<0.01	**	0.95 ± 0.23	0.90 ± 0.17	p<0.01	**
LVEDV (ml)	108.88 ± 25.49	92.21 ± 24.59	p<0.01	**	105.56 ± 25.84	96.44 ± 29.42	p<0.01	**
LV Mass d (gm)	128.46 ± 36.16	102.84 ± 30.99	p<0.01	**	158.93 ± 44.79	139.24 ± 38.15	p<0.01	**
CO (L/min)	5.29 ± 1.44	4.94 ± 1.72	p<0.01	**	5.16 ± 1.57	4.88 ± 1.55	p<0.01	**
E/A ratio	1.58 ± 0.60	1.40 ± 0.52	p<0.01	**	1.08 ± 0.41	1.09 ± 0.89	p<0.01	**
TDI E'	11.61 ± 5.96	9.86 ± 6.72	p<0.01	**	9.68 ± 2.55	9.06 ± 2.84	p<0.01	**
TDI E/E' ratio	0.16 ± 0.24	0.28 ± 0.40	p>0.05	NS	0.26 ± 0.81	0.19 ± 0.23	p<0.05	*
2D-EF(%)	62.62 ± 7.04	65.82 ± 7.61	p<0.01	**	65.25 ± 7.40	66.93 ± 8.18	p<0.01	**
2D-FS (%)	10.07 ± 17.09	9.15 ± 14.99	p<0.01	**	36.10 ± 5.61	37.44 ± 6.40	p<0.01	**
Variables	Categories			p				
	Category 1 (N-152)		Pooled category (N-348)	value		sign.		
	mn ± sd		mn ± sd					
GLS (%)	-19.03 ± 3.14		-17.33 ± 3.16	0.00000005		p<0.001		
GCS								
at mv level (%)	-15.91 ± 6.06		-15.34 ± 7.22	0.40		p>0.05		
at pap level (%)	-23.27 ± 6.81		-21.38 ± 8.25	0.01		p 0.01		
GRS								
at mv level (%)	21.88 ± 10.25		22.34 ± 11.19	0.67		p>0.05		
at pap level (%)	25.67 ± 11.32		25.49 ± 10.89	0.87		p>0.05		

GCSR				
at mv level (1/ sec)	-2.17 ± 0.69	-2.05 ± 1.79	0.43	p>0.05
at pap level (1/ sec)	-2.22 ± 1.75	-2.01 ± 0.76	0.06	BS
GRSR				
at mv level (1/ sec)	3.14 ± 0.97	3.29 ± 2.57	0.49	p>0.05
at pap level (1/ sec)	2.72 ± 0.96	2.75 ± 1.26	0.78	p>0.05

sd, standard deviation; sign, significance; M, male; F, female; mn, mean; HR, heart rate; n, number; SBP, systolic BP; DBP, diastolic BP; EPSS, E point septal separation; CO, cardiac output; 2D, two dimensional; EF, ejection fractional; FS, fractional shortening; sign, significance; *, significant; **, highly significant; NS, not significant; mn, mean; sd, standard deviation; sign, significance; GLS, global longitudinal strain; GCS, global circumferential strain; GRS, global radial strain; GCSR, global circumferential strain rate; GRSR, global radial strain rate; mv, mitral valve; pap, papillary muscle; BS, borderline significant.

Table1: Demographic, Conventional Echocardiography & Strain Data

Trend Analysis of Multiple Left Ventricular Strain Parameters

Trend analysis of MLVSP across ascending CVRF categories (Table 2, Figure 4) demonstrated a strong and statistically significant downward trajectory in GLS and GCS at the pap level (p < 0.01), indicating progressive deterioration in myocardial deformation with increasing cardiovascular risk. GCSR at the mv level also exhibited a mild yet statistically significant decline (p < 0.05), whereas GCSR at the papillary level showed borderline significance (p = 0.09). Other parameters, including radial strain and their respective strain rates, did not display significant trends (p > 0.05), suggesting relative preservation of these strain dimensions across risk categories.

Variables	Category 1 (n=152)	Category 2 (n 130)	Category 3 (n 143)	Category 4 (n 75)	Trend\p value	sign.
	mn ± sd	mn ± sd	mn ± sd	mn ± sd		
GLS(%)	-19.03 ± 3.14	-16.33 ± 2.17	-15.99 ± 3.53	-14.09 ± 1.58	p=0.001	p<0.01
GCS						
at mv level (%)	-15.91 ± 6.06	-14.95 ± 6.96	-15.37 ± 7.98	-15.62 ± 5.94	p=0.70	p>0.05
at pap level (%)	-23.27 ± 6.81	-21.32 ± 8.05	-20.32 ± 8.32	-20.31 ± 7.81	p=0.005	p<0.01
GRS						
at mv level (%)	21.88 ± 10.25	23.16 ± 11.81	21.77 ± 10.73	21.94 ± 10.82	p=0.71	p>0.05
at pap level (%)	25.67 ± 11.32	25.05 ± 10.84	24.46 ± 10.93	24.91 ± 10.31	p=0.82	p>0.05
GCSR						
at mv level (1/sec)	-2.14 ± 0.79	-1.99 ± 0.65	-1.94 ± 0.69	-1.92 ± 0.62	p=0.04	p<0.05
at pap level (1/sec)	-2.22 ± 1.75	-2.01 ± 0.89	-1.96 ± 0.64	-1.86 ± 0.65	p=0.09	BS
GRSR						
at mv level (1/sec)	3.14 ± 0.97	3.09 ± 1.19	3.59 ± 3.77	2.96 ± 0.93	p=0.13	p>0.05
at pap level (1/sec)	2.72 ± 0.96	2.70 ± 1.23	2.81 ± 1.41	2.75 ± 1.33	p=0.87	p>0.05

sd, standard deviation; sign, significance; BS, borderline significance; GLS, global longitudinal strain; GCS, global circumferential strain; GRS, global radial strain; GCSR, global circumferential strain rate; GRSR, global radial strain rate; mv, mitral valve; pap, papillary muscle.

Table2: Trend of LV strain parameters in cardiovascular risk factor categories

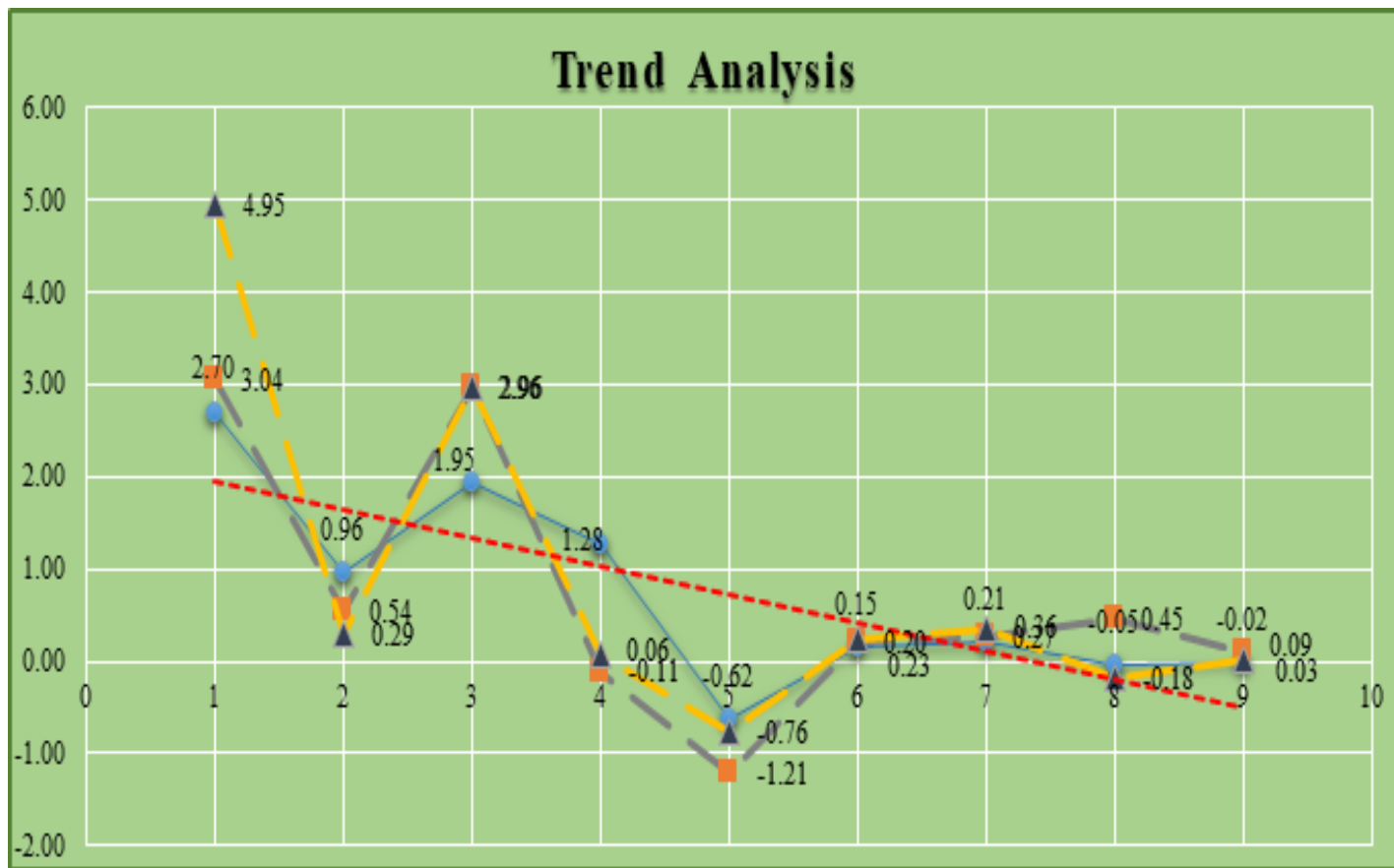


Figure4: Graphical illustration of the trend analysis of MLVSP across cardiovascular risk categories 1–4, highlighting the progressive decline in GLS and GCS at pap level with increasing risk burden.

Pearson’s Correlation (Bivariate Analysis)

Pearson’s correlation analysis revealed predominantly weak to moderate linear relationships among the strain parameters, suggesting generally mild associations (Table 3, Figure 5):

- **Moderate negative correlations** were observed between:
 - GCS and GRS at the mv level ($r = -0.463$)
 - GCS and GRS at the pap level ($r = -0.528$)

These findings suggest a notable inverse relationship, wherein increased GCS may correspond with reduced GRS at the respective anatomical levels.

- Most of the remaining correlations were **weakly positive or weakly negative**, indicating limited linear dependency among the majority of strain parameters.

Despite the small effect sizes, **several of these correlations were statistically significant**, as supported by corresponding *p-values*.

		GLS (%)	GCS mv level	GCS pap level	GRS mv level	GRS pap level	GCSR mv level	GCSR pap level	GRSR mv level	GRSR pap level
GLS (%)	r	1	0.013	0.180	-0.045	-0.063	0.070	0.113	0.034	0.012
	Sig. (2-tailed)		0.764	0.0001	0.318	0.161	0.116	0.011	0.443	0.793
GCS mv level	r	0.013	1	0.300	-0.463	-0.166	0.252	0.082	-0.085	-0.092
	Sig. (2-tailed)	0.764		0.0000000001	0.000000000000000001	0.0002	0.0000000001	0.066	0.057	0.039

GCS pap level	r	0.180	0.3	1	-0.136	-0.528	0.198	0.359	-0.002	-0.113
	Sig. (2-tailed)	0.0001	0.00000 000001		0.002	0.0000000 00000000 00000000 00000000 0000003	0.00001	0.0000 000000 000001	0.963	0.011
GRS mv level	r	-0.045	-0.463	-0.136	1	0.219	-0.171	-0.007	0.121	-0.034
	Sig. (2-tailed)	0.318	0.000000 0000000 0000000 0000001	0.002		0.000001	0.0001	0.880	0.007	0.442
GRS pap level	r	-0.063	-0.166	-0.528	0.219	1	-0.093	-0.149	-0.078	0.141
	Sig. (2-tailed)	0.161	0.0002	0.000000 00000000 00000000 00000000 0000003	0.000001		0.038	0.001	0.081	0.002
GCSR mv level	r	0.070	0.252	0.198	-0.171	-0.093	1	0.194	-0.262	-0.104
	Sig. (2-tailed)	0.116	0.000 00001	0.00001	0.0001	0.038		0.00001	0.0000 00003	0.020
GCSR pap level	r	0.113	0.082	0.359	-0.007	-0.149	0.194	1	-0.055	-0.216
	Sig. (2-tailed)	0.011	0.066	0.000000 0000000 001	0.880	0.001	0.00001		0.224	0.0000 01
GRSR mv level	r	0.034	-0.085	-0.002	0.121	-0.078	-0.262	-0.055	1	0.130
	Sig. (2-tailed)	0.443	0.057	0.963	0.007	0.081	0.0000 00003	0.224		0.004
GRSR pap level	r	0.012	-0.092	-0.113	-0.034	0.141	-0.104	-0.216	0.13	1
	Sig. (2-tailed)	0.793	0.039	0.011	0.442	0.002	0.020	0.000 001	0.004	

	Strong Negative Correlations	$r \leq -0.70$
	Moderate Negative Correlations	$r = -0.40$ to -0.69
	Weak Negative Correlations	$r = -0.10$ to -0.39
	Weak Positive Correlations	$r = +0.10$ to $+0.39$
	Moderate Positive Correlations	$r = +0.40$ to $+0.69$
	Strong Positive Correlations	$r \geq +0.70$

GLS, global longitudinal strain; GCS, global circumferential strain; GRS, global radial strain; GCSR, global circumferential strain rate; GR SR, global radial strain rate; mv, mitral valve; pap, papillary muscle; sig., significance;

Table3: Pearson’s correlation coefficient (Bivariate analysis)

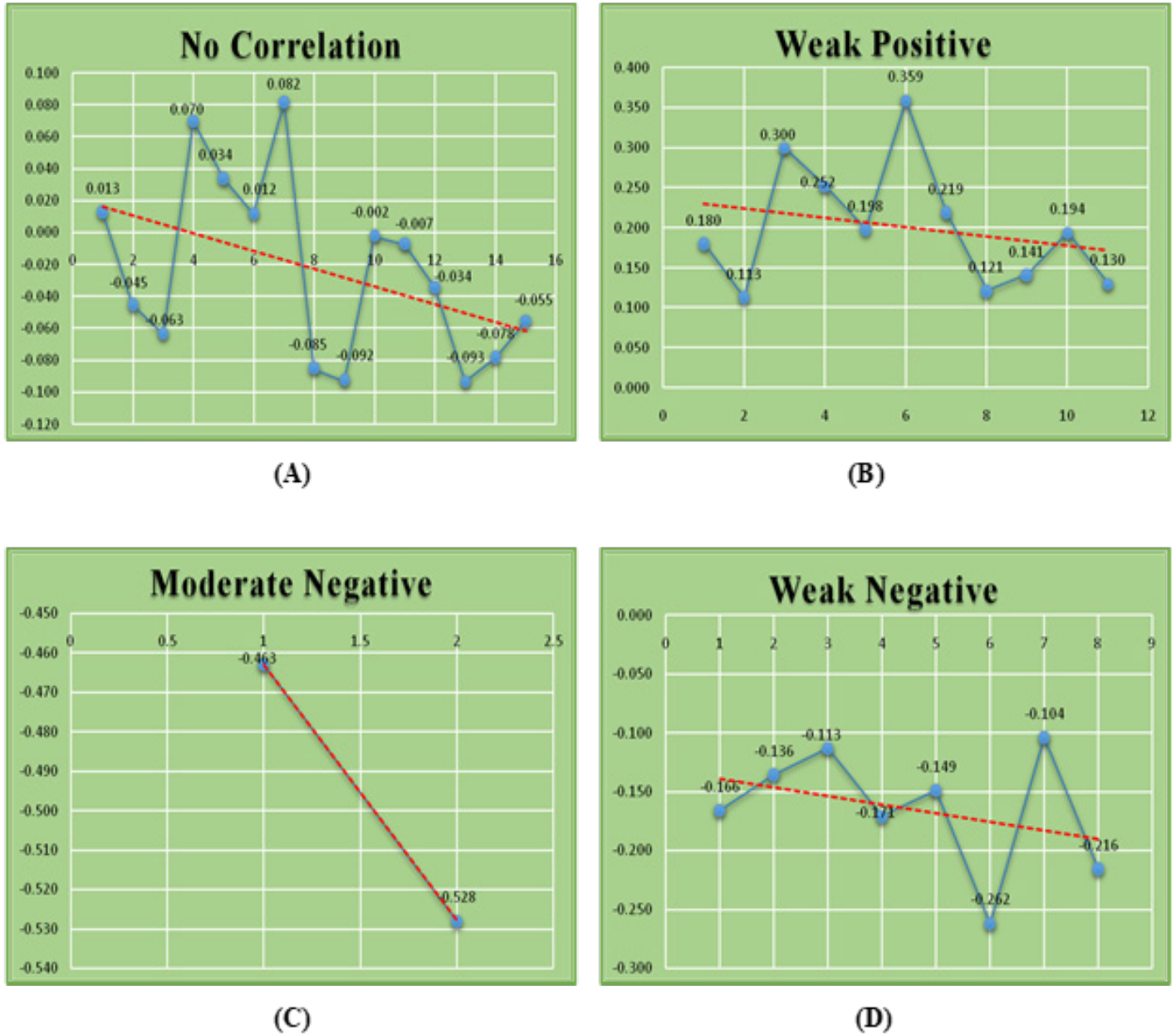


Figure 5: Pearson's correlation: (A), No correlation; (B), Weak Positive; (C), Moderate Negative; (D), Weak Negative.

Multivariate Regression Analysis

On multivariate regression analysis, the following significant associations were identified (Table 4, Figure 6):

- Risk Category 3 – GLS ($\beta = -0.164, p = 0.043$),
- Risk Category 2 – GCSR at mv level ($\beta = -0.174, p = 0.032$), and
- Risk Category 4 – GCSR at mv level ($\beta = -0.188, p = 0.021$),

all demonstrated statistically significant associations with Risk Category 1 – GLS.

Other LV strain parameters did not exhibit any independent significant associations.

Parameters		Multivariate (β)	Correlations	p-values
GLS (%)	Risk category 2	0.130	0.126	0.109
	Risk category 3	-0.164	-0.160	* 0.043
	Risk category 4	-0.068	-0.064	0.397
GCS mv level	Risk category 2	0.69	0.103	0.410
	Risk category 3	-0.103	-0.125	0.214
	Risk category 4	-0.102	-0.122	0.215
GCS pap level	Risk category 2	0.056	0.070	0.499
	Risk category 3	-0.124	-0.131	0.138
	Risk category 4	-0.007	-0.018	0.933
GRS mv level	Risk category 2	-0.027	-0.032	0.745
	Risk category 3	0.045	0.048	0.588
	Risk category 4	0.034	0.033	0.677
GRS pap level	Risk category 2	-0.121	-0.144	0.144
	Risk category 3	-0.038	-0.025	0.641
	Risk category 4	0.037	0.032	0.654
GCSR mv level	Risk category 2	-0.174	-0.151	* 0.032
	Risk category 3	-0.027	-0.026	0.733
	Risk category 4	0.188	0.168	* 0.021
GCSR pap level	Risk category 2	0.033	0.029	0.693
	Risk category 3	0.025	0.021	0.768
	Risk category 4	0.011	0.010	0.896
GRSR mv level	Risk category 2	0.080	0.079	0.331
	Risk category 3	-0.010	-0.008	0.905
	Risk category 4	0.075	0.075	0.359
GRSR pap level	Risk category 2	-0.002	-0.003	0.981
	Risk category 3	0.038	0.038	0.644
	Risk category 4	0.018	-0.017	0.828

GLS, global longitudinal strain; GCS, global circumferential strain; GRS, global radial strain; GCSR, global circumferential strain rate; GRSR, global radial strain rate; mv, mitral valve; pap, papillary muscle; *, $p < 0.05$.

Table 4: Multivariate regression analysis

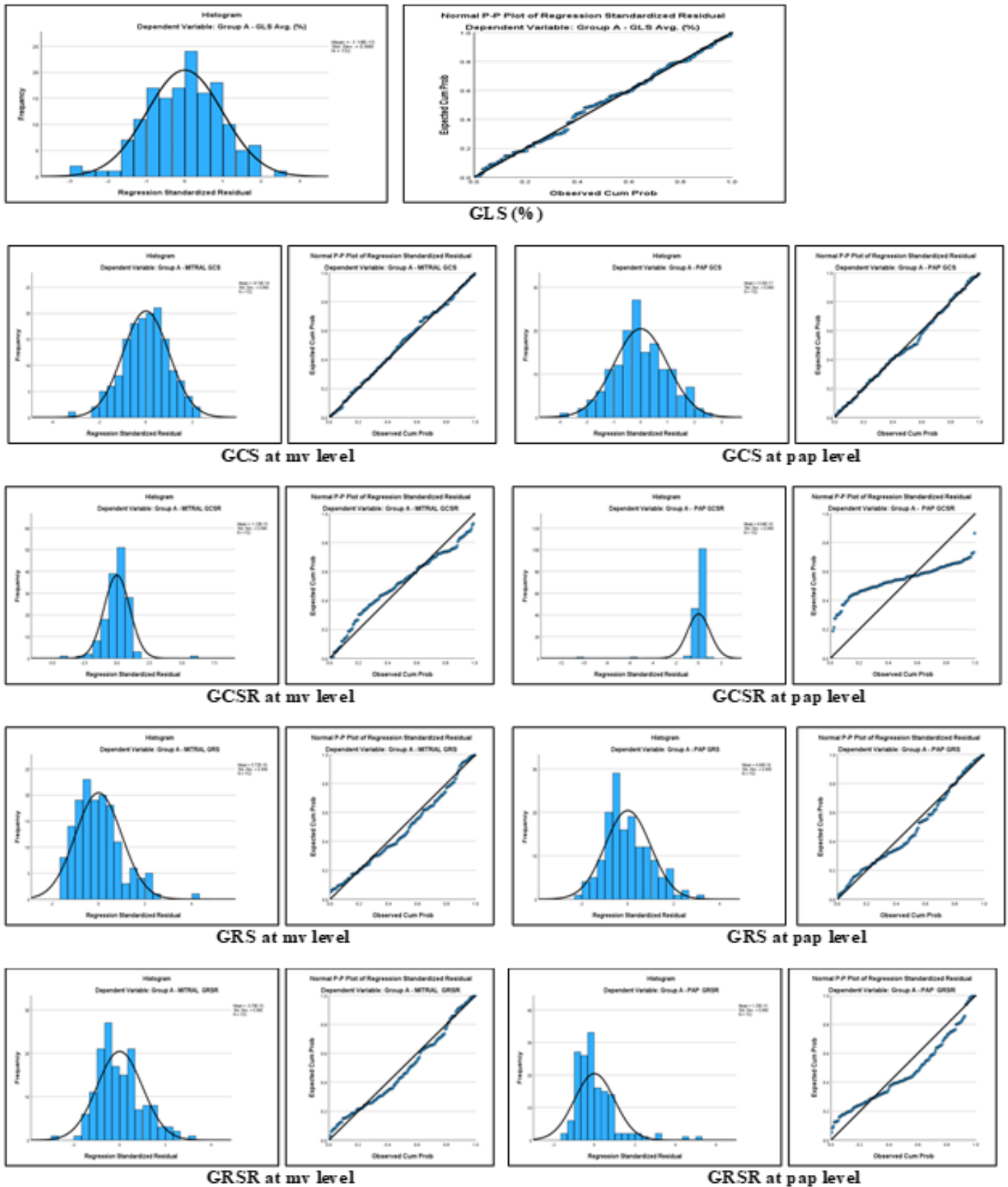


Figure6: Graphical Illustration of multivariate regression analysis of MLVSP across risk categories.

Discussion

Two-dimensional speckle tracking echocardiography (2D STE) remains a widely employed, non-invasive modality for evaluating left ventricular (LV) systolic function, as well as strain, volumetric indices, and rotational mechanics—including twist, torsion, and rotation [17,18]. However, inherent limitations persist across 2D, 3D, and 4D STE platforms [17]. The most recent innovation, XStrain™ 4D, was developed to improve the precision of LV contractile function assessment [17], although its adoption in routine clinical practice remains limited.

4Dimensional/3Dimensional versus 2Dimensional Speckle Tracking Echocardiography

Prior studies have demonstrated that real-time three-dimensional echocardiography (RT3DE) and four-dimensional STE (4D STE) offer superior accuracy in quantifying LV ejection fraction (LVEF) and strain parameters compared to conventional 2D echocardiography [19-21]. This advantage largely stems from the geometric assumptions inherent to 2D-derived LVEF calculations [22]. Indeed, several reports have shown that LVEF and LV volumes measured by 2D imaging tend to be overestimated relative to RT3DE or 4D modalities [23, 24]. In the present study, we employed 4DXStrainSTE to perform LVEF and volumetric assessments within a true 3D/4D analytical framework.

Earlier work by Takahashi et al. [9] and the STAAB cohort [25] examined the influence of CVRFs on LV strain using 2D echocardiographic platforms. However, 2D-based methods may compromise strain accuracy due to spatial and geometric limitations. In contrast, our study leveraged 4DXStrainSTE—a technologically advanced and potentially more precise modality [7,26].

Clinical Significance of Cardiovascular Risk Factors on LV Strain

GLS has emerged as a sensitive and prognostically valuable marker of adverse cardiovascular outcomes, often surpassing GCS and GRS in predictive capacity. This superiority likely reflects the vulnerability of subendocardial, longitudinally oriented myocardial fibers to early pathological insults during the initial stages of myocardial dysfunction [27,28]. Conversely, circumferential strain-reflecting mid-wall circumferential fibers—typically remains preserved until later disease stages [29]. Radial strain, representing myocardial wall thickening in the radial dimension, is comparatively less sensitive to early changes [30]. Strain rate parameters provide complementary insights into the velocity of myocardial deformation, thereby refining the characterization of contraction and relaxation kinetics.

CVRFs are highly prevalent among older adults and, if unaddressed, predispose individuals to overt cardiovascular disease (CVD) [31]. The cumulative presence of multiple CVRFs has been implicated in the development of subclin-

ical myocardial dysfunction [32]. Importantly, impaired GLS has been reported even in individuals with preserved LVEF, underscoring its value as an early marker of myocardial impairment [33]. Moreover, multiple studies have linked an increasing burden of CVRFs with stepwise elevations in cardiovascular mortality risk [34,35].

Although prior investigations have explored the relationship between CVRFs and strain—primarily GLS—using 2D STE [9,25], our study, employing 4DXStrainSTE, detected significantly lower GLS and GCS at the papillary level in pooled CVRF categories compared with the low-risk group ($p < 0.01$). While reductions in GCS at the mitral level, GRS at both mitral and papillary levels, and GRSR were also observed in the CVRF group, these differences did not achieve statistical significance ($p > 0.05$).

Furthermore, trend analysis and linearity testing via Pearson's correlation and multivariate regression demonstrated a significant, progressive decline in GLS and GCS at the papillary level across ascending CVRF categories, consistent with worsening myocardial deformation. GCSR at the papillary level showed borderline significance ($p = 0.09$). Pearson's bivariate correlation revealed predominantly mild linear associations among strain indices, while multivariate regression identified significant associations between GLS and GCSR at the mitral level with GLS.

GLS remains the most widely adopted strain parameter in both clinical and research settings [36]. However, there is a notable paucity of studies systematically evaluating the impact of CVRFs on GCS and GRS. To our knowledge, this is the first study to comprehensively examine the clinical implications of CVRFs on GCS, GRS, GCSR, and GRSR using an advanced 4DXStrainSTE platform.

Conclusion

This study provides comprehensive normative data on LV strain parameters in healthy Indian adults and individuals with CVRFs, assessed using advanced 4DXStrainSTE. The presence of CVRFs was significantly associated with reduced GLS and GCS at the papillary level ($p < 0.01$), while GCSR at the papillary level showed a borderline reduction ($p = 0.06$). In contrast, GRSR values were marginally higher but not statistically significant ($p > 0.05$).

A robust statistical approach—including trend analysis, Pearson's correlation, and multivariate regression—demonstrated that ascending CVRF categories were associated with a significant stepwise decline in GLS and GCS at the papillary level ($p < 0.01$), GCSR at the mitral level ($p < 0.05$), and borderline significance for GCSR at the papillary level ($p = 0.09$), indicating progressive myocardial dysfunction. Other parameters showed non-significant or inconsistent patterns ($p > 0.05$). Pearson's correlation revealed predominantly mild linear associations among strain parameters, while mul-

tivariate regression identified significant associations of GLS and GCSR at the mitral level with GLS.

To the best of our knowledge, this is the first single-center investigation to comprehensively evaluate MLVSP in the context of CVRFs using 4DXStrainSTE. The results highlight distinct differences in LV strain profiles between CVRF-affected individuals and healthy controls, supporting the clinical utility of XStrain™ 4D STE as a cost-effective and sensitive tool for detailed ventricular mechanics assessment, particularly for GLS and related strain parameters.

Limitations of the Present Research

1. This was a single-center study conducted on healthy Indian adults. Therefore, the reference values generated cannot be extrapolated to other ethnic groups such as Africans, Europeans, or Americans.
2. The specific ultrasound system used plays a significant role in strain evaluation, and values may differ when using other echocardiographic platforms due to software algorithm variability [37].
3. A major limitation lies in the lack of standardization of GLS values across vendors, which can affect strain measurements [38,39].
4. The study did not incorporate validation against cardiac magnetic resonance tagging (CMR-TAG) or feature tracking (CMR-FT) [40], which remain the gold standards for strain analysis.

References

1. Yingchoncharoen, Teerapat, Shikhar Agarwal, Zoran B. Popović, and Thomas H. Marwick. "Normal ranges of left ventricular strain: a meta-analysis." *Journal of the American Society of Echocardiography* 26, no. 2 (2013): 185-191.
2. Lang RM, Badano LP, Mor-Avi V, Afilalo J, Armstrong A, Ernande L, Flachskampf FA, Foster E, Goldstein SA, Kuznetsova T, Lancellotti P, Muraru D, Picard MH, Rietzschel ER, Rudski L, Spencer KT, Tsang W, Voigt JU. Recommendations for cardiac chamber quantification by echocardiography in adults: an update from the American Society of Echocardiography and the European Association of Cardiovascular Imaging. *J Am Soc Echocardiogr.* 2015; 28:1-39.
3. Jasaityte, Ruta, Brecht Heyde, and Jan D'hooge. "Current state of three-dimensional myocardial strain estimation using echocardiography." *Journal of the American Society of Echocardiography* 26, no. 1 (2013): 15-28.
4. Papademetris, Xenophon, Albert J. Sinusas, Donald P. Dione, and James S. Duncan. "Estimation of 3D left ventricular deformation from echocardiography." *Medical image analysis* 5, no. 1 (2001): 17-28.
5. Elen, An, Hon Fai Choi, Dirk Loeckx, Hang Gao, Piet Claus, Paul Suetens, Frederik Maes, and Jan D'hooge. "Three-dimensional cardiac strain estimation using spatio-temporal elastic registration of ultrasound images: A feasibility study." *IEEE transactions on medical imaging* 27, no. 11 (2008): 1580-1591.
6. Muraru, Denisa, Alice Niero, Hugo Rodriguez-Zanella, Diana Cherata, and Luigi Badano. "Three-dimensional speckle-tracking echocardiography: benefits and limitations of integrating myocardial mechanics with three-dimensional imaging." *Cardiovascular diagnosis and therapy* 8, no. 1 (2018): 101.
7. Takahashi, Ken, Ghassan Al Naami, Richard Thompson, Akio Inage, Andrew S. Mackie, and Jeffrey F. Smallhorn. "Normal rotational, torsion and untwisting data in children, adolescents and young adults." *Journal of the American Society of Echocardiography* 23, no. 3 (2010): 286-293.
8. Muraru, Denisa, Umberto Cucchini, Sorina Mihăilă, Marcelo Haertel Miglioranza, Patrizia Aruta, Giacomo Cavalli, Antonella Cecchetto et al. "Left ventricular myocardial strain by three-dimensional speckle-tracking echocardiography in healthy subjects: reference values and analysis of their physiologic and technical determinants." *Journal of the American Society of Echocardiography* 27, no. 8 (2014): 858-871.
9. Takahashi, Tomonori, Kenya Kusunose, Robert Zheng, Natsumi Yamaguchi, Yukina Hirata, Susumu Nishio, Yoshihito Saijo et al. "Association between cardiovascular risk factors and left ventricular strain distribution in patients without previous cardiovascular disease." *Journal of Echocardiography* 20, no. 4 (2022): 208-215.
10. Al Saikhan, Lamia, Chloe Park, Rebecca Hardy, and Alun Hughes. "Prognostic implications of left ventricular strain by speckle-tracking echocardiography in population-based studies: a systematic review protocol of the published literature." *BMJ open* 8, no. 7 (2018): e023346.
11. Unger, Thomas, Claudio Borghi, Fadi Charchar, Nadia A. Khan, Neil R. Poulter, Dorairaj Prabhakaran, Agustin Ramirez et al. "Clinical practice guidelines." *Hypertension* 75 (2020): 1334-1357.
12. National Cholesterol Education Program (NCEP) Expert Panel on Detection, Evaluation, and Treatment of High Blood Cholesterol in Adults (Adult Treatment Panel III). Third Report of the National Cholesterol Education Program (NCEP) Expert Panel on Detection, Evaluation, and Treatment of High Blood Cholesterol in Adults (Adult Treatment Panel III) final report. *Circulation.* 2002;106:3143-421.
13. WHO expert consultation. Appropriate body-mass index for Asian populations and its implications for policy and intervention strategies. *Lancet.* 2004;36:3157-63.
14. American Diabetes Association. Standards of Medical Care in Diabetes-2020. *Diabetes Care.* 2020;43:S1-S212.

15. Marston, Louise, James R. Carpenter, Kate R. Walters, Richard W. Morris, Irwin Nazareth, Ian R. White, and Irene Petersen. "Smoker, ex-smoker or non-smoker? The validity of routinely recorded smoking status in UK primary care: a cross-sectional study." *BMJ open* 4, no. 4 (2014): e004958.
16. Mitchell, Carol, Peter S. Rahko, Lori A. Blauwet, Barry Canada, Joshua A. Finstuen, Michael C. Foster, Kenneth Horton, Kofo O. Ogunyankin, Richard A. Palma, and Eric J. Velazquez. "Guidelines for performing a comprehensive transthoracic echocardiographic examination in adults: recommendations from the American Society of Echocardiography." *Journal of the American Society of Echocardiography* 32, no. 1 (2019): 1-64.
17. Mehrotra, Akhil, Anurag Mehrotra, Mohammed Shaban, and Shubham Kacker. "Four-Dimensional XStrain Echocardiographic Assessment of Left Ventricular Strain and Rotational Mechanics: Technology, Clinical Applications, Advantages and Limitations." *Cardiovascular Innovations and Applications* 9, no. 1 (2024): 968.
18. Mehrotra, Akhil, Shubham Kacker, Mohammad Shadab, Naveen Chandra, and Alok Kumar Singh. "4 Dimensional XStrain speckle tracking echocardiography: comprehensive evaluation of left ventricular strain and twist parameters in healthy Indian adults during COVID-19 pandemic." *American Journal of Cardiovascular Disease* 12, no. 4 (2022): 192.
19. Chen, Ran, Xia Wu, Li-Jun Shen, Bei Wang, Ming-Ming Ma, Yuan Yang, and Bo-Wen Zhao. "Left ventricular myocardial function in hemodialysis and nondialysis uremia patients: a three-dimensional speckle-tracking echocardiography study." *PLoS One* 9, no. 6 (2014): e100265.
20. Zhu, Meihua, Cole Streiff, Jill Panosian, Zhijun Zhang, Xubo Song, David J. Sahn, and Muhammad Ashraf. "Regional strain determination and myocardial infarction detection by three-dimensional echocardiography with varied temporal resolution." *Echocardiography* 32, no. 2 (2015): 339-348.
21. Jenkins, Carly, Kristen Bricknell, Lizelle Hanekom, and Thomas H. Marwick. "Reproducibility and accuracy of echocardiographic measurements of left ventricular parameters using real-time three-dimensional echocardiography." *Journal of the American College of Cardiology* 44, no. 4 (2004): 878-886.
22. Chen, Ran, Meihua Zhu, David J. Sahn, and Muhammad Ashraf. "Non-invasive evaluation of heart function with four-dimensional echocardiography." *PLoS one* 11, no. 5 (2016): e0154996.
23. Patted, Suresh V., Sameer Ambar, Sanjay C. Porwal, Prabhu C. Halkati, M. R. Prasad, Vijay B. Metgudmath, Vishwanath Hesarur, Vaibhav Patil, M. Anand Kumar, and Shakuntala Chitrali. "Comparison of left ventricular volume and left ventricular ejection fraction by 2-dimensional echocardiography by Simpson's method & real time 3-dimensional echocardiography in patients of normal conduction with normal left ventricular function, complete left bundle branch block with normal left ventricular function and with left ventricular dysfunction." *Journal of Indian College of Cardiology* 8, no. 4 (2018): 167-171.
24. Al-Allak, Hanan Mohsen Ali, and Asaad Hasan Noaman Al-Aboodi. "A Four-Dimensional Volumetric Quantification of the Left Ventricle in Healthy Pregnant Women in the Third Trimester." *Cureus* 15, no. 10 (2023).
25. Morbach, Caroline, Bettina N. Walter, Margret Breunig, Dan Liu, Theresa Tiffe, Martin Wagner, Götz Gelbrich, Peter U. Heuschmann, Stefan Störk, and STAAB consortium. "Speckle tracking derived reference values of myocardial deformation and impact of cardiovascular risk factors—Results from the population-based STAAB cohort study." *PLoS one* 14, no. 9 (2019): e0221888.
26. van Mil, Anke CCM, James Pearson, Aimee L. Drane, John R. Cockcroft, Barry J. McDonnell, and Eric J. Stoehr. "Interaction between left ventricular twist mechanics and arterial haemodynamics during localised, non-metabolic hyperaemia with and without blood flow restriction." *Experimental Physiology* 101, no. 4 (2016): 509-520.
27. Delgado, Victoria, Laurens F. Tops, Rutger J. Van Bommel, Frank Van Der Kley, Nina Ajmone Marsan, Robert J. Klautz, Michel IM Versteegh, Eduard R. Holman, Martin J. Schalij, and Jeroen J. Bax. "Strain analysis in patients with severe aortic stenosis and preserved left ventricular ejection fraction undergoing surgical valve replacement." *European heart journal* 30, no. 24 (2009): 3037-3047.
28. Lindqvist, Per, Gani Bajraktari, Roberta Molle, Elizabetta Palmerini, Anders Holmgren, Sergio Mondillo, and Michael Y. Henein. "Valve replacement for aortic stenosis normalizes sub-endocardial function in patients with normal ejection fraction." *European Journal of Echocardiography* 11, no. 7 (2010): 608-613.
29. Greenbaum, R. A., S. Yen Ho, D. G. Gibson, A. E. Becker, and RH7008815 Anderson. "Left ventricular fibre architecture in man." *Heart* 45, no. 3 (1981): 248-263.
30. Rahaman, Sk Affur, Ranjit K. Nath, Abhishek Kumawat, Bhusan Madhukar Tile, Sk Affur Rahaman, Ranjit K. Nath, Abhishek Kumawat, and Bhusan Madhukar Tile. "A Comparative Study of Detection of Alteration of Left Ventricular Strain by Speckle Tracking Echocardiography in Adult Patients with Rheumatic Mitral Stenosis." *European Journal of Cardiovascular Medicine* 14 (2024): 307-313.
31. Matsuoka, Mitsuteru, Taku Inoue, Tetsuji Shinjo, Asuka Miiji, Masahiro Tamashiro, Kageyuki Oba, Hisatomi Arima, and Osamu Arasaki. "Cardiovascular risk profile and frailty in Japanese outpatients: the Nambu Cohort Study." *Hypertension Research* 43, no. 8 (2020): 817-823.
32. Lloyd-Jones DM, Braun LT, Ndumele CE, et al. Use of risk assessment tools to guide decision-making in the primary prevention of atherosclerotic cardiovascular disease: a special report from the American Heart Association and American College of Cardiology. *Circulation*. 2019;139:e1162-e1177.
33. Edvardsen, Thor, Thomas Helle-Valle, and Otto A. Smiseth. "Systolic dysfunction in heart failure with normal ejection fraction: speckle-tracking echocardiography." *Progress in cardiovascular diseases* 49, no. 3 (2006): 207-214.

34. Li, Dongze, Yu Jia, Jing Yu, Yi Liu, Fanghui Li, Yanmei Liu, Qinqin Wu et al. "Adherence to a healthy lifestyle and the risk of all-cause mortality and cardiovascular events in individuals with diabetes: the ARIC study." *Frontiers in Nutrition* 8 (2021): 698608.
35. Barr, Elizabeth LM, Paul Z. Zimmet, Timothy A. Welborn, Damien Jolley, Dianna J. Magliano, David W. Dunstan, Adrian J. Cameron et al. "Risk of cardiovascular and all-cause mortality in individuals with diabetes mellitus, impaired fasting glucose, and impaired glucose tolerance: the Australian Diabetes, Obesity, and Lifestyle Study (AusDiab)." *Circulation* 116, no. 2 (2007): 151-157.
36. Zhang, Kan, Richard Sheu, Nicole M. Zimmerman, Andrej Alfirevic, Shiva Sale, A. Marc Gillinov, and Andra E. Duncan. "A comparison of global longitudinal, circumferential, and radial strain to predict outcomes after cardiac surgery." *Journal of cardiothoracic and vascular anesthesia* 33, no. 5 (2019): 1315-1322.
37. Patrianakos, Alexandros P., Aggeliki A. Zacharaki, Antonios Kalogerakis, Georgios Solidakis, Fragiskos I. Parthenakis, and Panos E. Vardas. "Two-dimensional global and segmental longitudinal strain: are the results from software in different high-end ultrasound systems comparable?." *Echo Research & Practice* 2, no. 1 (2015): 29-39.
38. Nelson, Matthew R., R. Todd Hurst, Serageldin F. Raslan, Stephen Cha, Susan Wilansky, and Steven J. Lester. "Echocardiographic measures of myocardial deformation by speckle-tracking technologies: the need for standardization?." *Journal of the American Society of Echocardiography* 25, no. 11 (2012): 1189-1194.
39. Thomas, James D., and Luigi P. Badano. "EACVI-ASE-industry initiative to standardize deformation imaging: a brief update from the co-chairs." *European Heart Journal–Cardiovascular Imaging* 14, no. 11 (2013): 1039-1040.
40. Zweerink, Alwin, Cornelis P. Allaart, Joost PA Kuijjer, LiNa Wu, Aernout M. Beek, Peter M. van de Ven, Mathias Meine et al. "Strain analysis in CRT candidates using the novel segment length in cine (SLICE) post-processing technique on standard CMR cine images." *European Radiology* 27, no. 12 (2017): 5158-5168.